Quantitative shape analysis of intertesseral joints in tessellated calcified cartilage of sharks and rays (elasmobranchs)

Ronald Seidel[1], Ahmed Hosny[2], David Knötel[3], Peter Fratzl[1], Daniel Baum[3], James Weaver[2], Mason N. Dean[1]
[1] Max Planck Inst., Germany; [2] Wyss Inst., USA; [3] Zuse Inst., Germany

Introduction: Sharks & rays have armored skeletons, comprised of uncalcified cartilage covered by mineralised tiles (tesserae). The mechanical function of this skeletal tessellation remains unclear. We used high-resolution imaging and developed advanced 3D data processing tools to characterize how tesserae interact at ultrastructural levels, gaining insight into form-function relationships of their complex joints and their roles in whole skeletal element performance.

Shark & ray tessellated cartilage

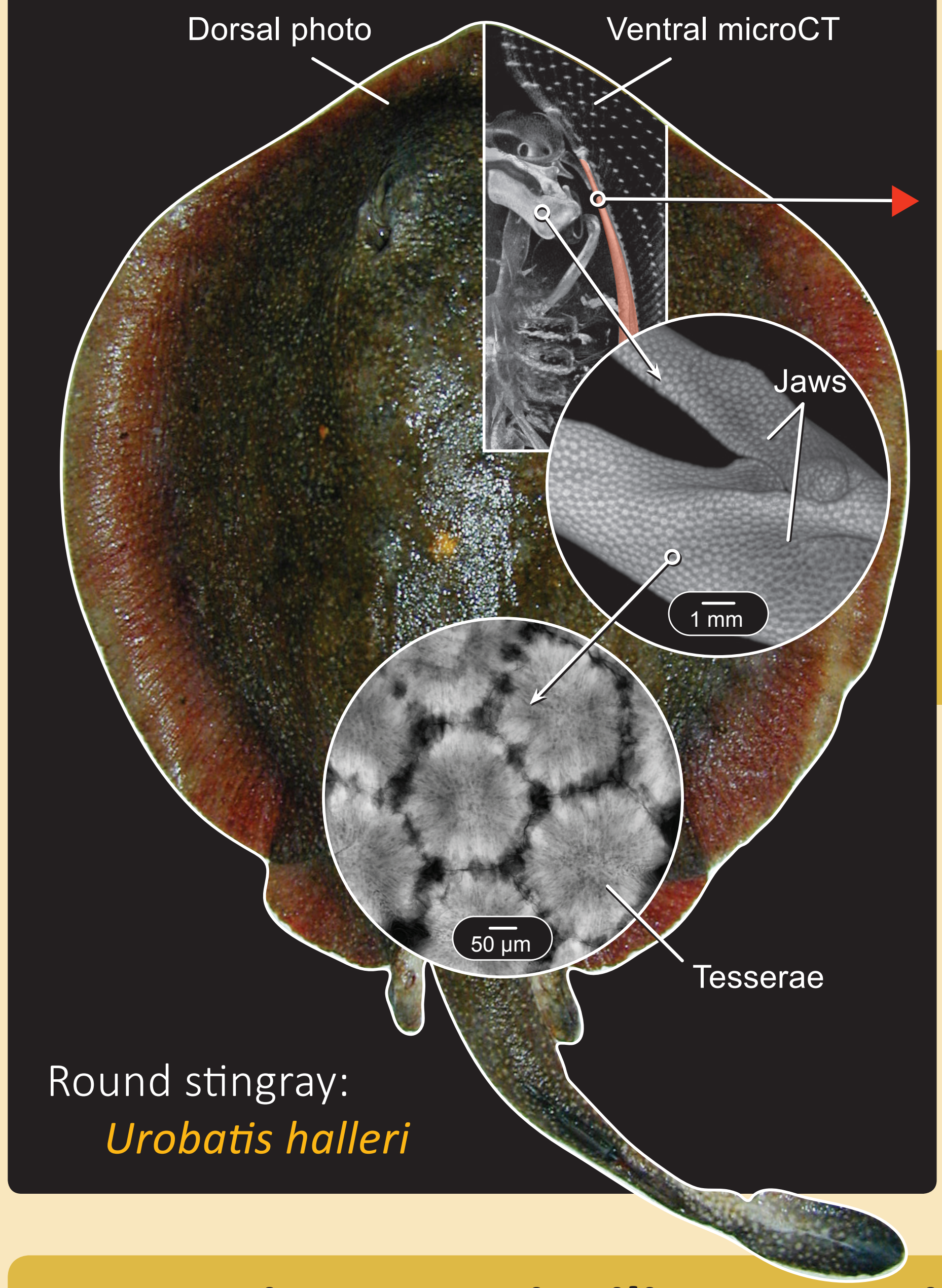

Round stingray:
Urobatis halleri

Characterizing ultrastructural features of tesserae and intertesseral joints

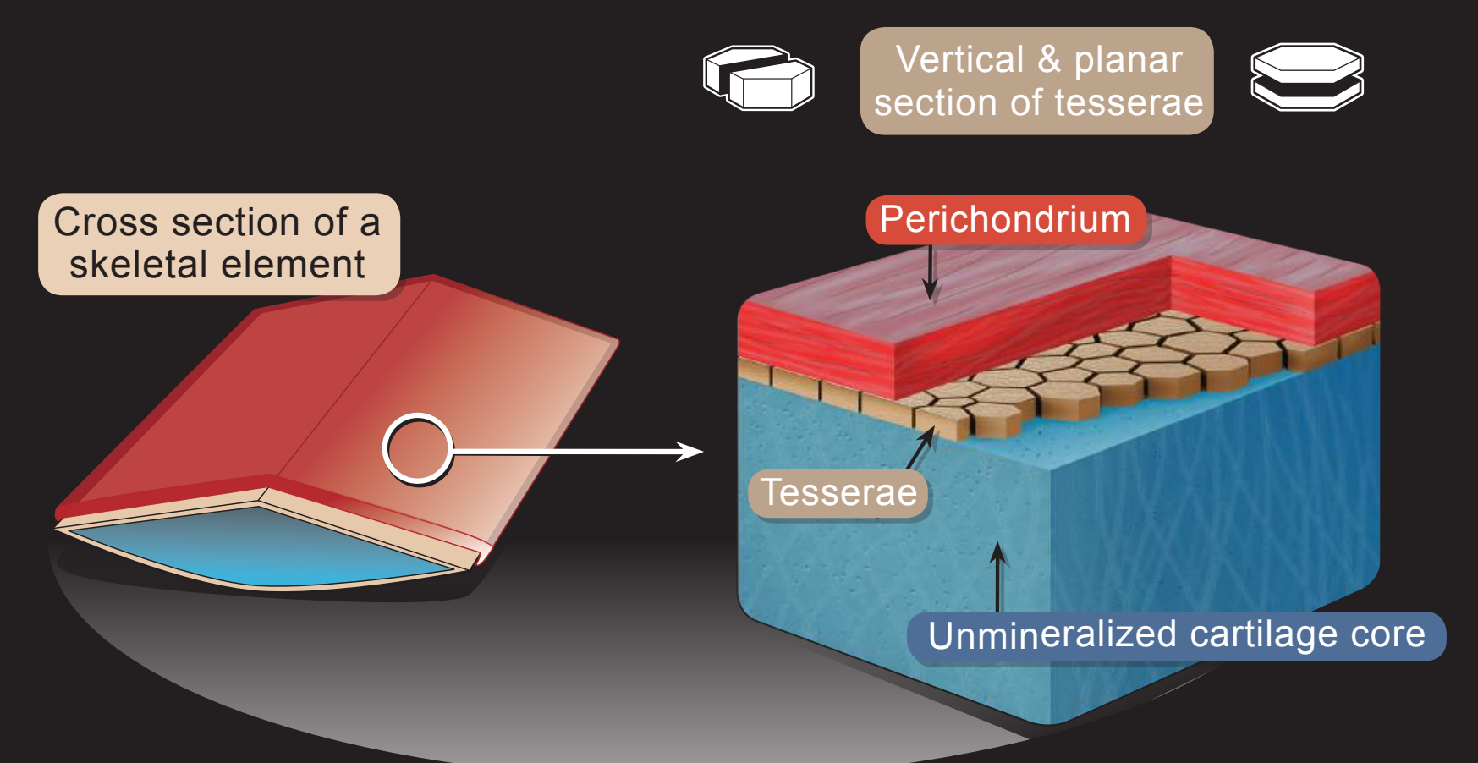

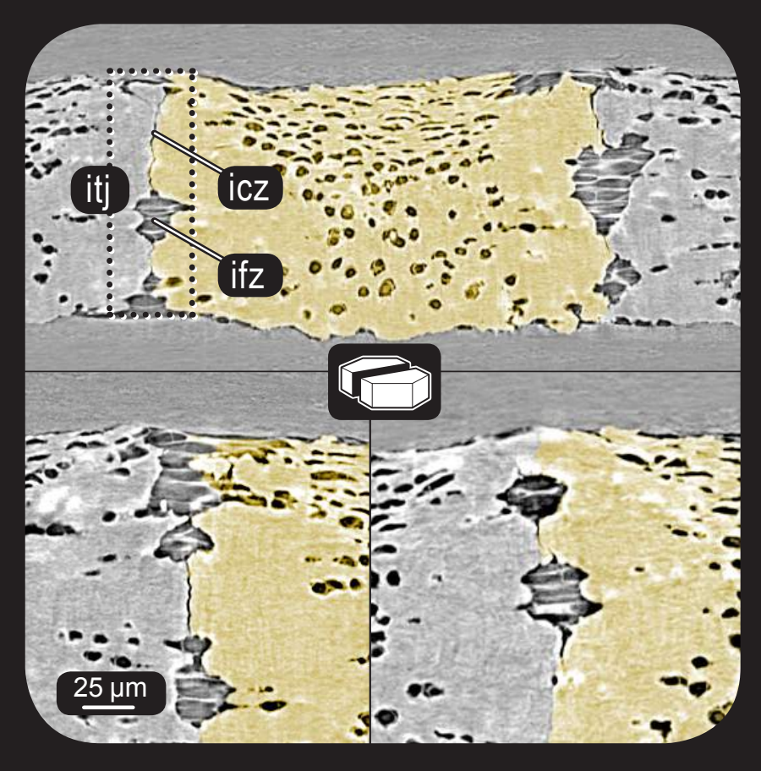

SR-microCT

Intertesseral joints appear rather flat in 2D virtual vertical sections.

3D reconstructions of the complex joint arrangment of fibrous attachment or contact zones.

SR-microCT

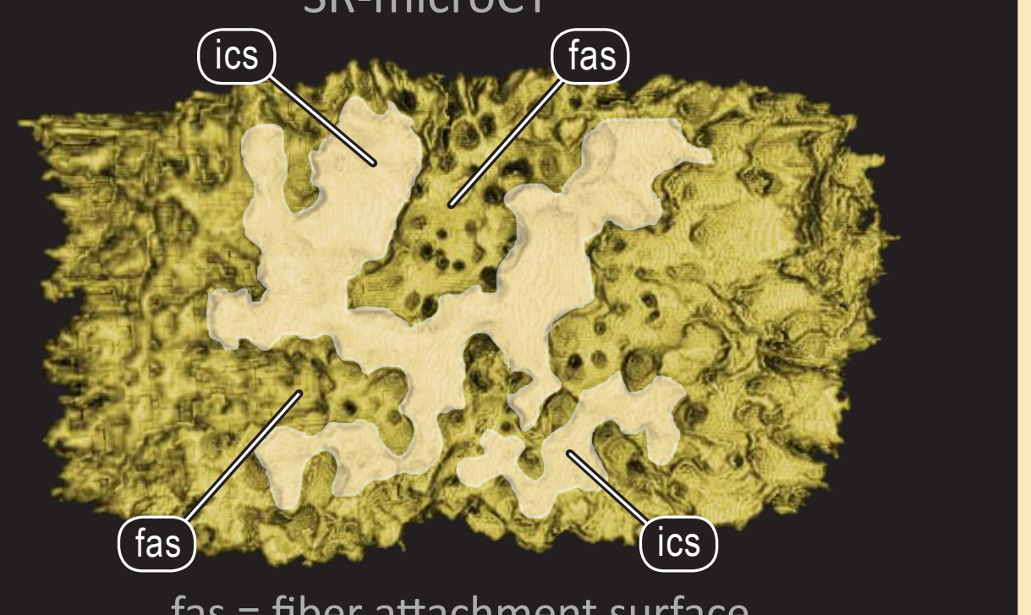

fas = fiber attachment surface
ics = intertesseral contact surface

Backscatter & Environmental Scanning Electron Microscopy

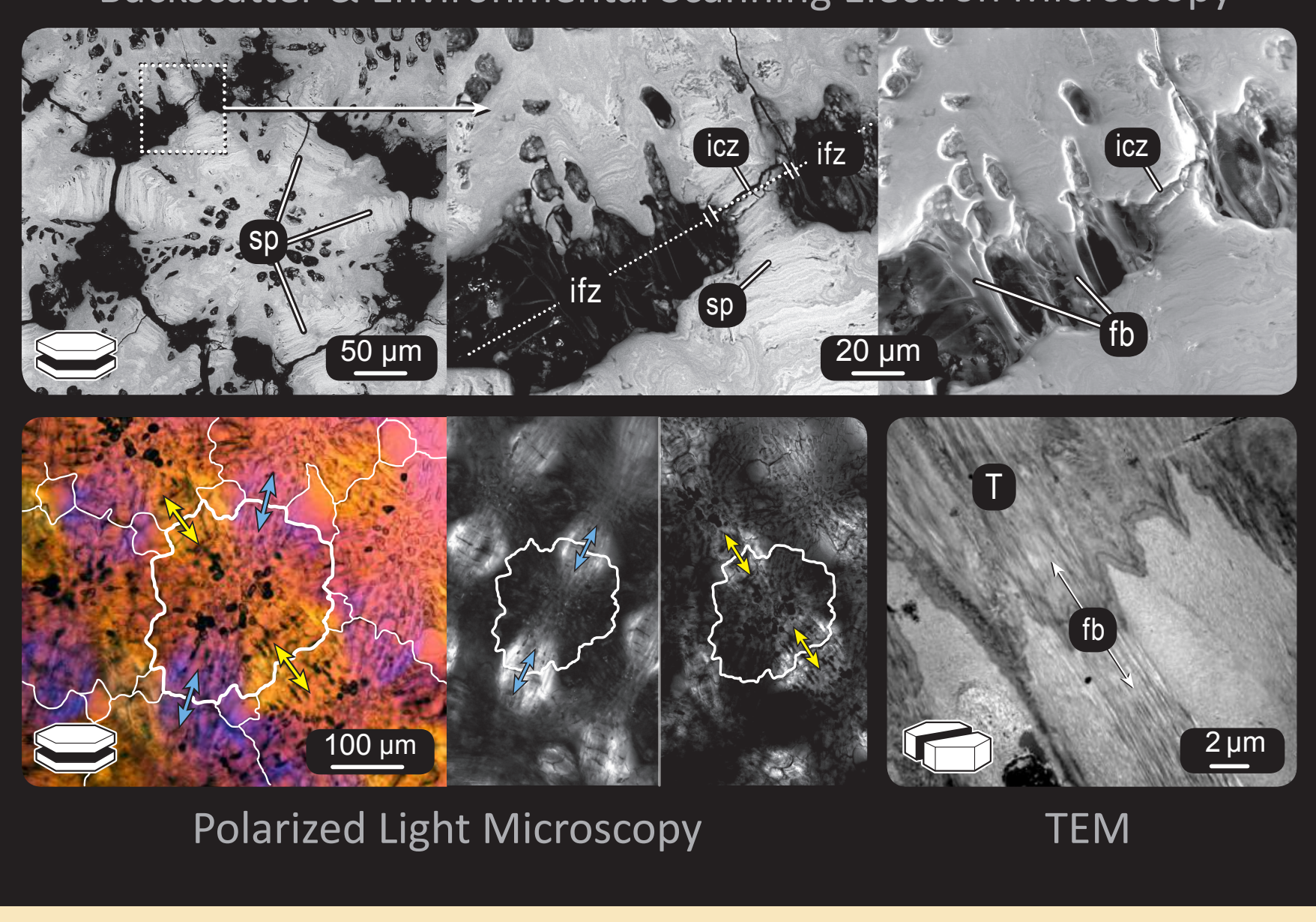

Polarized Light Microscopy TEM

Tesserae abut against one another forming contact zones, or are linked via unmineralized fibrous zones.

The collagenous joint fibers are firmly anchored in the mineralized matrix, forming flexible linkages.

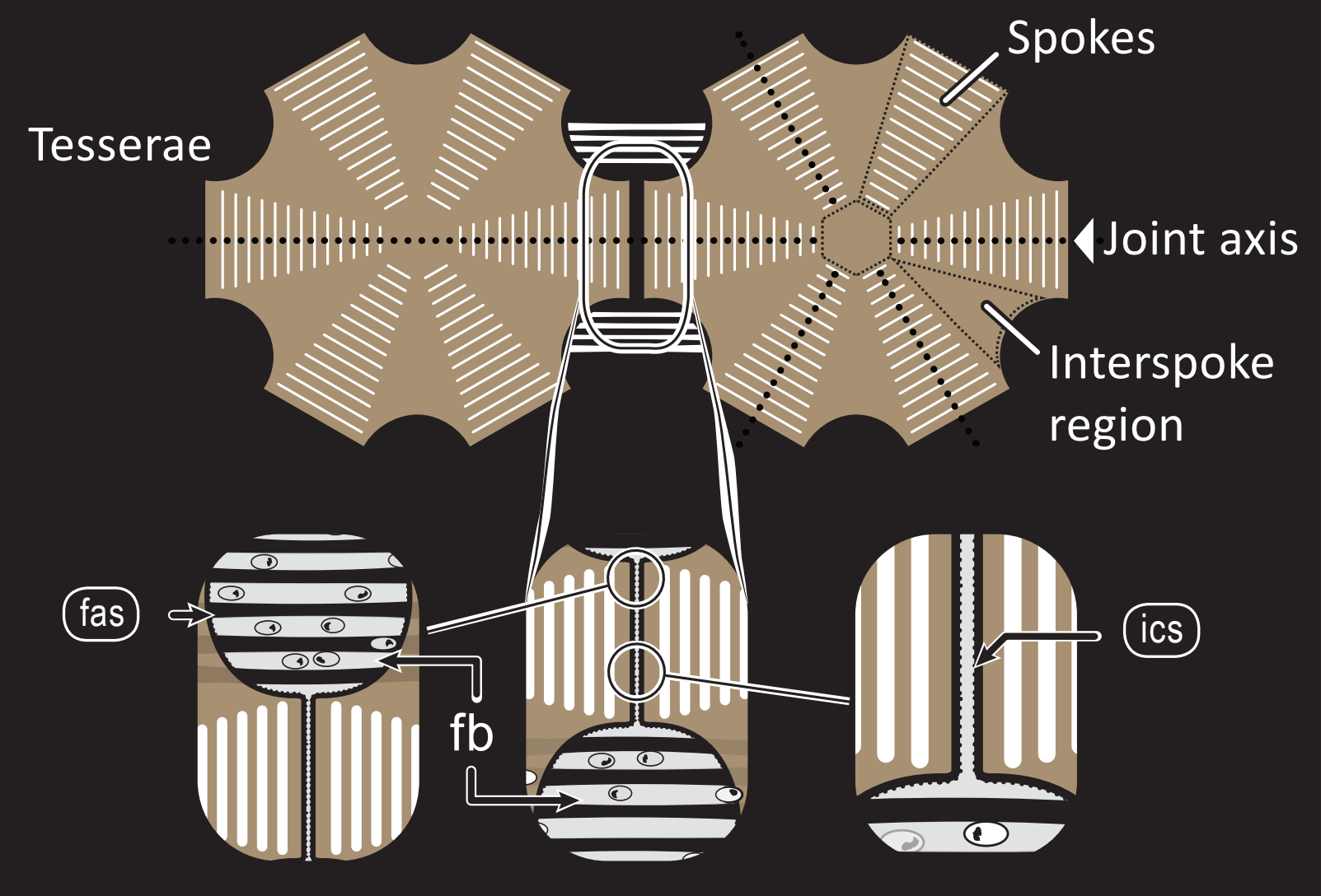

Intertesseral fibrous zone ITF

Intertesseral joint ITJ

Intertesseral contact zone ICZ

DOWNLOAD PUBLICATION

Semi-automatic tiling recognition of tesserae networks

TESSERAE SEGMENTATION PIPELINE

We developed custom modules for semi-automatic tiling-recognition using AmiraZIB Edition to segment individual tiles in microCT scans of tesseral mats and quantify tesserae shape variation across skeletal elements in 3D.

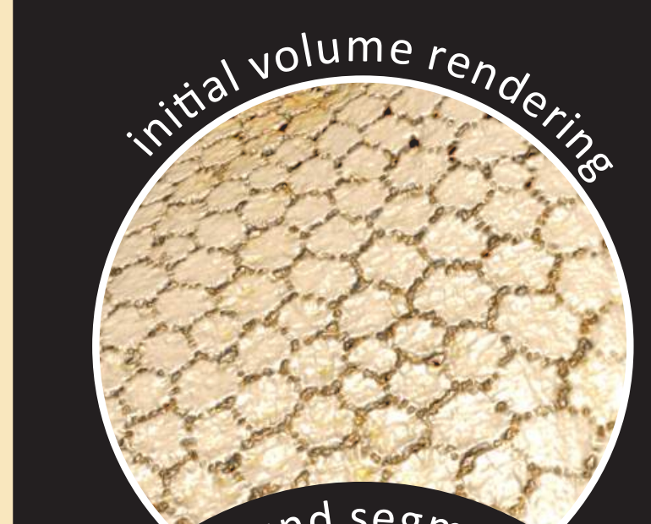

Heterogenous grey value distribution (e.g. high values at edges, lower values in centers)

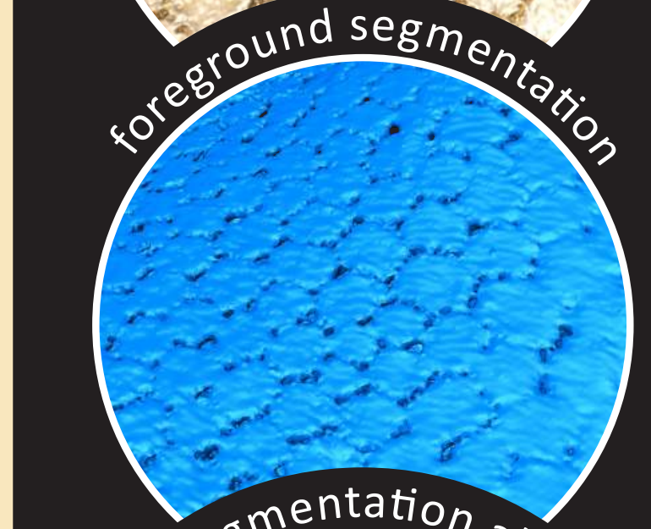

Binary segmentation separates tesserae from background

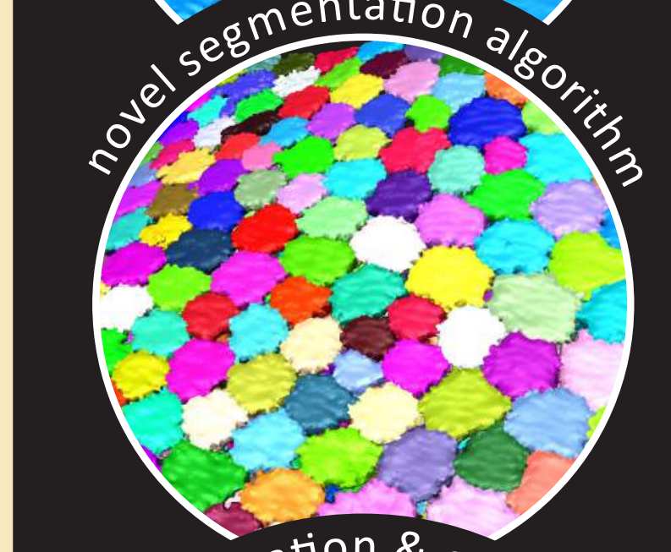

Individual tesserae separated by applying a hierarchical watershed segmentation to a 2D distance map

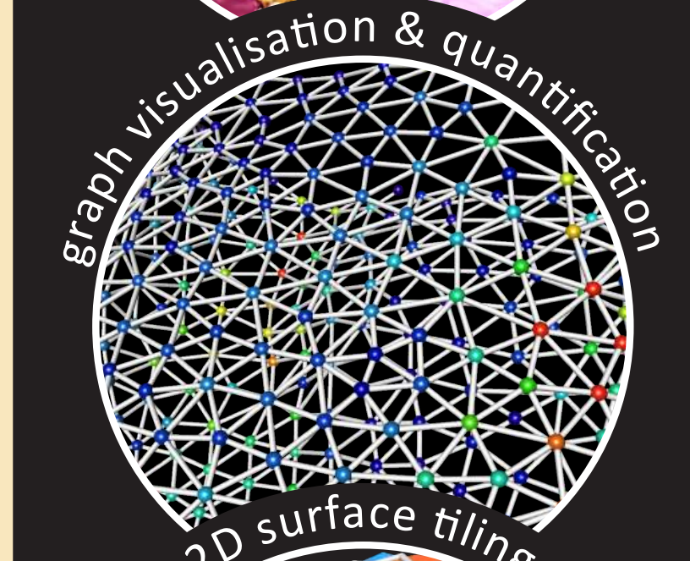

Statistical information computed per tessera used to annotate an abstract graph representation of the tesserae network

Tesserae network graph representation used to characterize 2D tilings of the skeletal element's surface

SKELETAL ELEMENT & TESSERAE SHAPE ANALYSIS

Visualisation of tesseral morphometrics allows comprehensive 3D analyses of the organisation of tesseral networks to define underlying principles of form-function relationships in the tiling pattern.

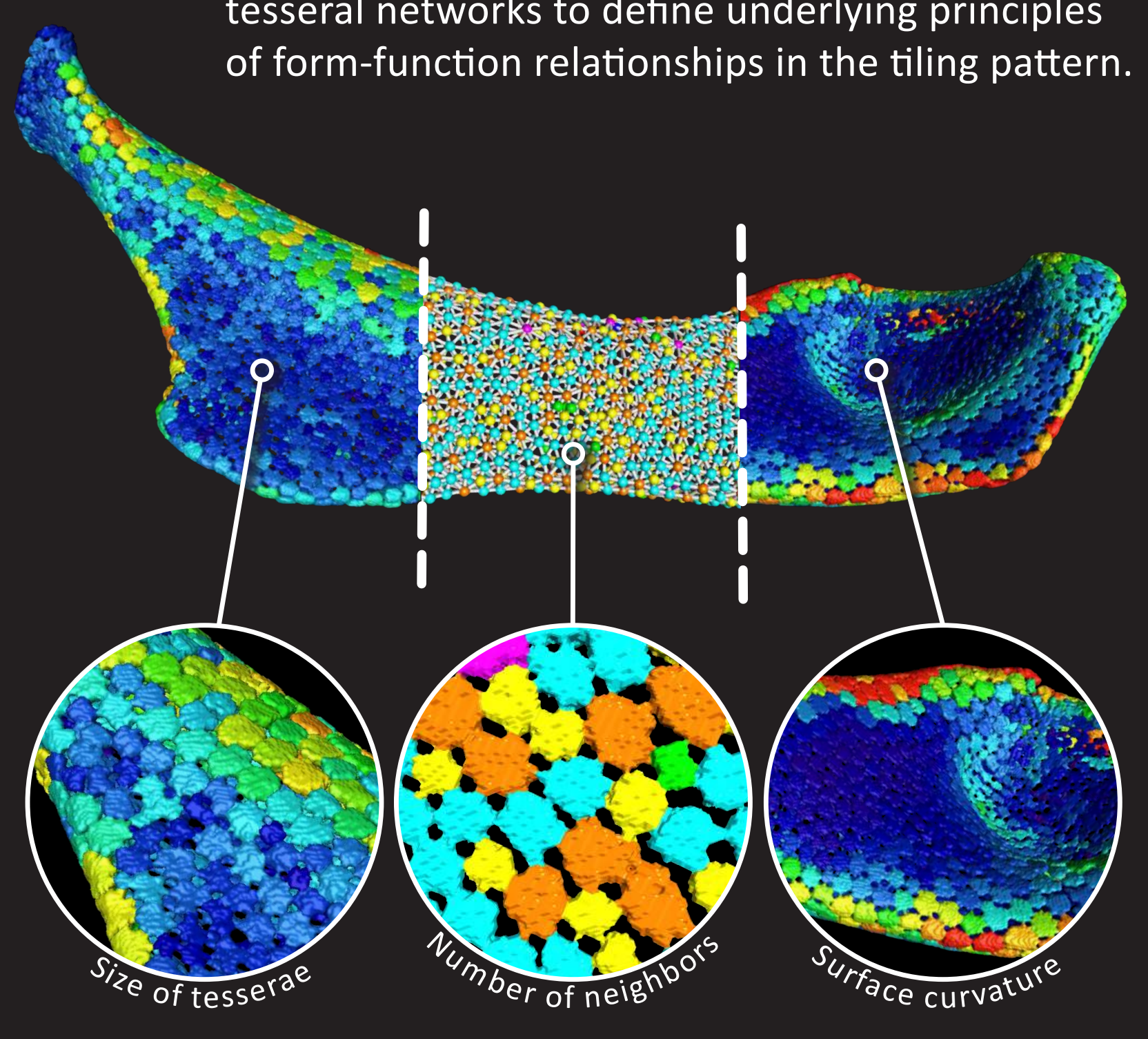

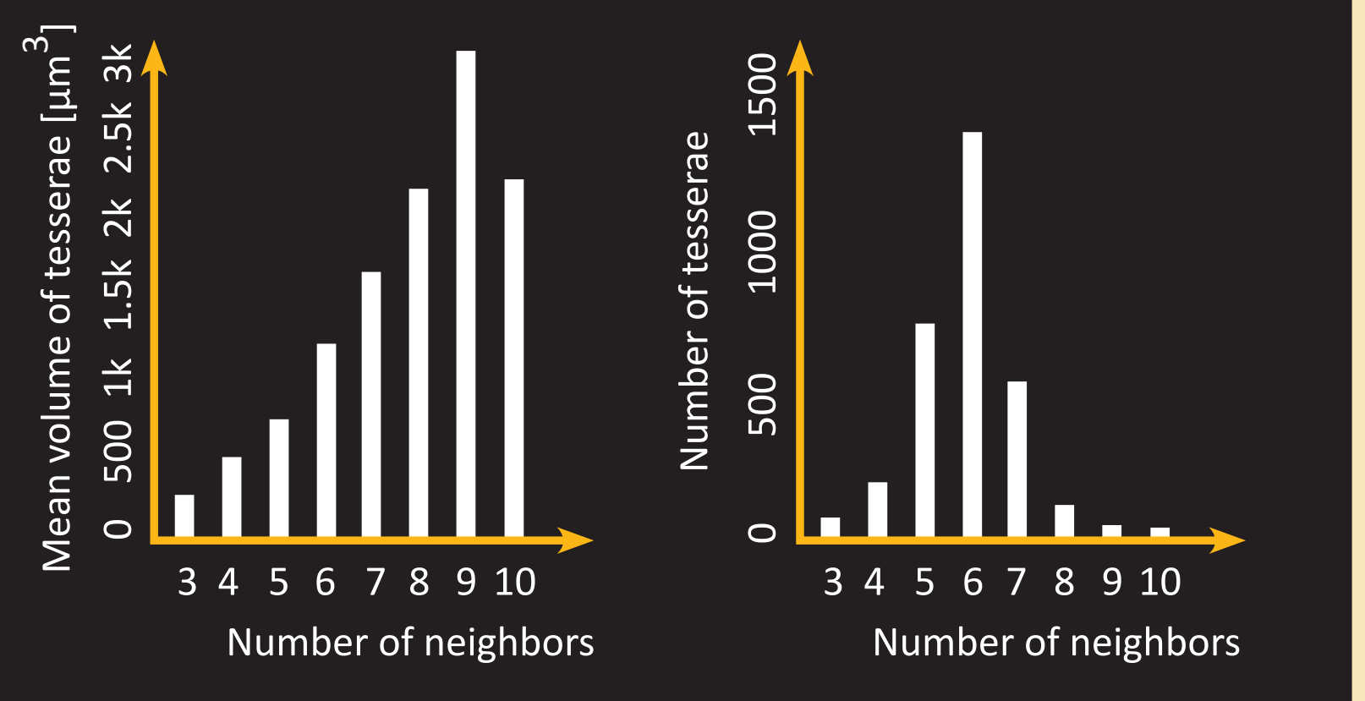

Knötel et al. 2017, *in prep.*

Companion/Future studies

3D prints enable testing of the degrees of freedom of intertesseral joints and...

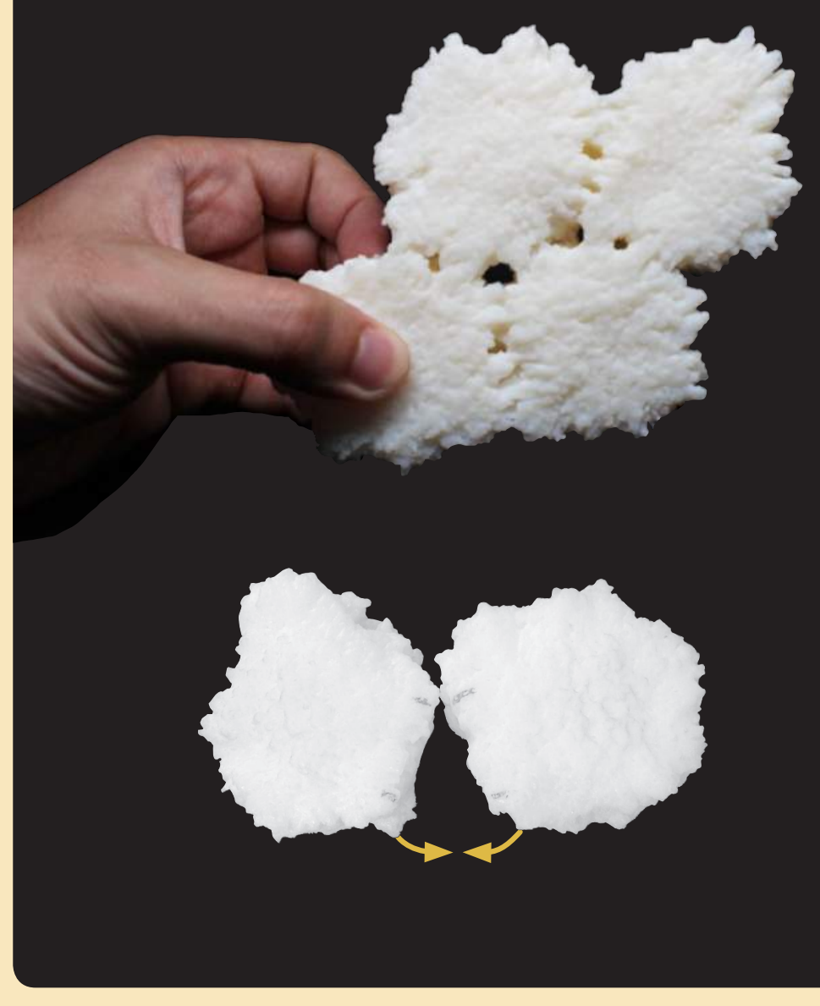

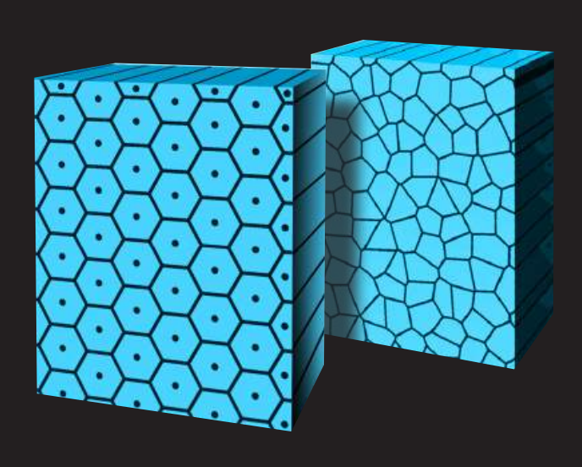

...allow us to perform material tests with physical models of bio-inspired tilings...

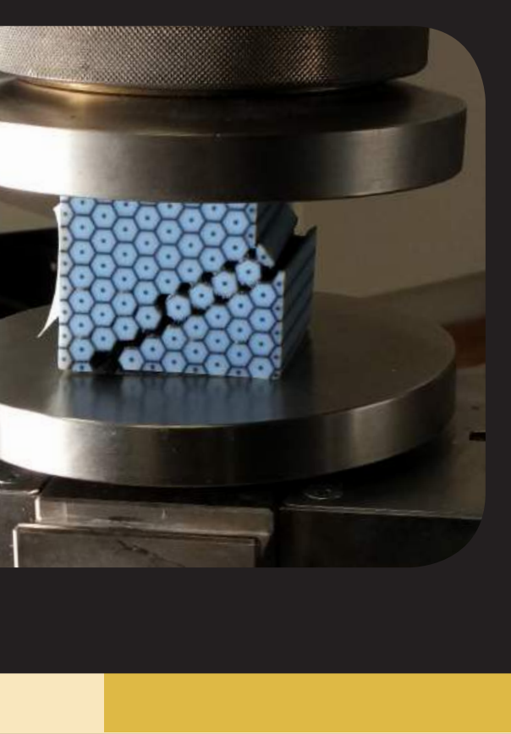

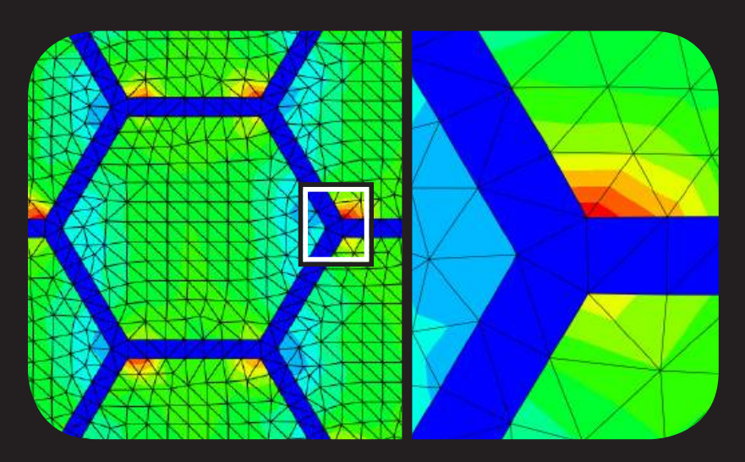

...the results of which can be verified by Finite Element Analyses of biomimicked tessellations (Jayasankar et al. 2017, *in press*)

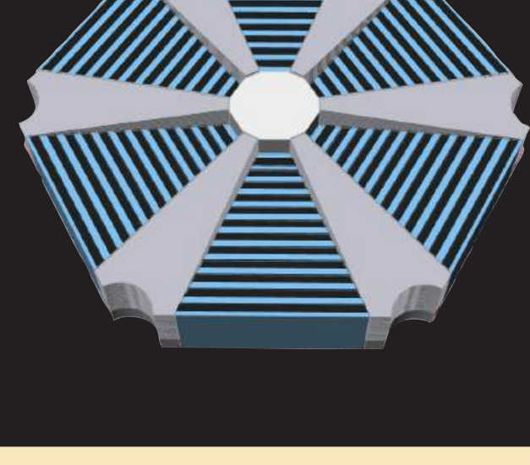

Mesh-based quantitative analysis of intertesseral joints

TESSERAE JOINT CHARACTERISATION PIPELINE

We developed an advanced shape-analysis-algorithm in Python to quantify tesserae interaction from microCT data by defining joint parameters, such as contact zones, joint flatness and interlocking. We present an exemplar data set; this technique will be applied to multiple joints in future work.

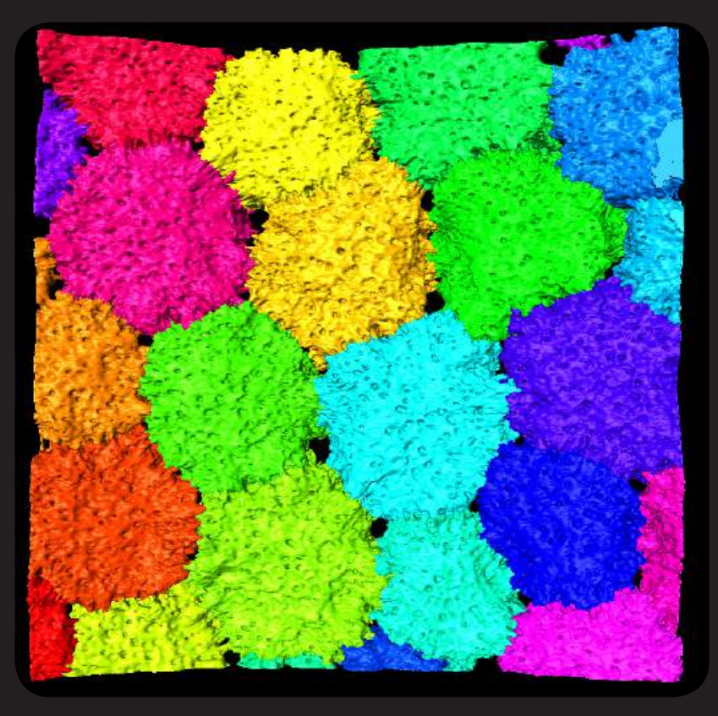

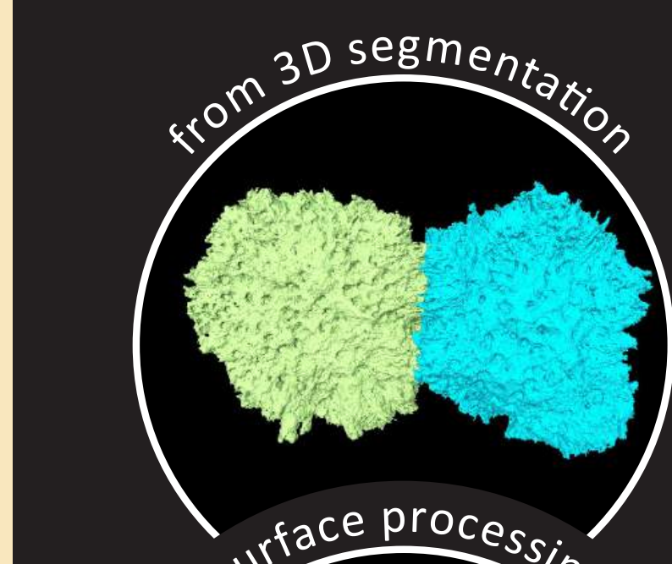

Neighboring tesserae (T1&2) segmented and their surface geometries described by a triangle mesh

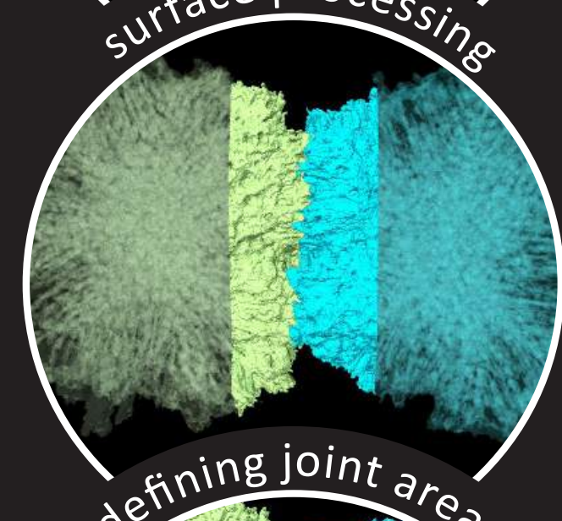

Surfaces cut to isolate relevant region and to reduce vertices and faces for faster computation

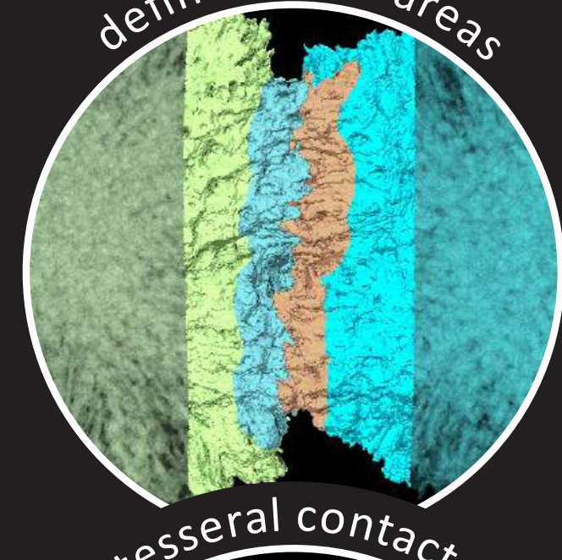

Joint region defined by a 30µm ROI enclosing opposing tesseral surfaces and the space between them

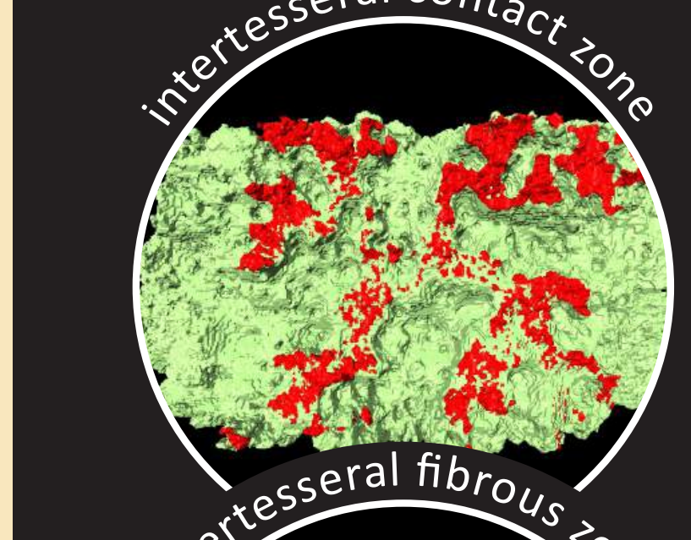

T1&2 mesh regions in close proximity (≤2 µm) were identified as contact zones.

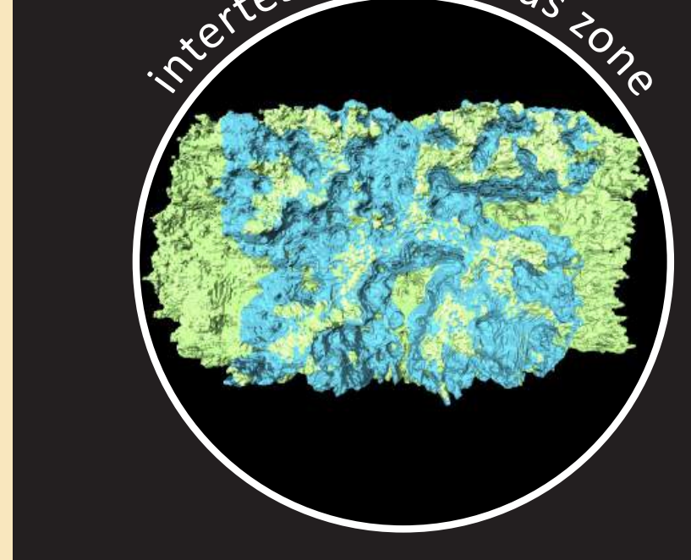

Remaining T1&2 mesh regions within the 30µm ROI were identified as fibrous zones

DEFINING JOINT SYMMETRY VIA THE *BEST FIT PLANE* 'BFP'

A "best fit plane" bisects T1&2 joint space, allowing calculation of intrusion, separation and flatness of tesseral edges.

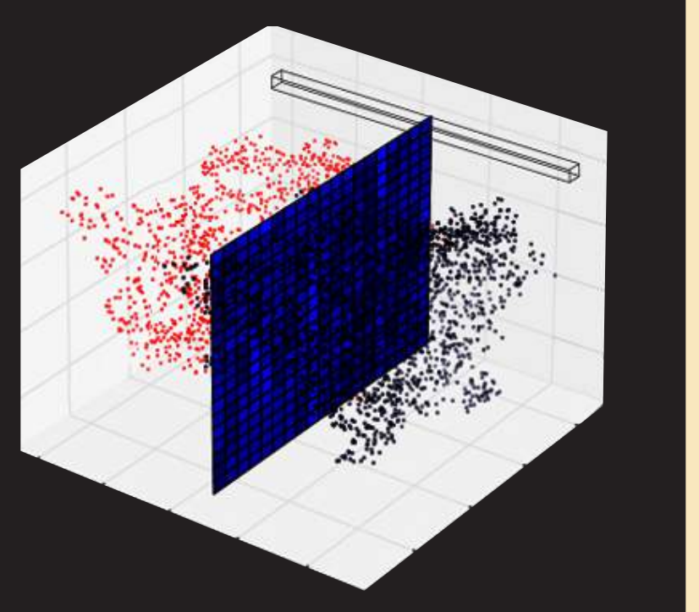

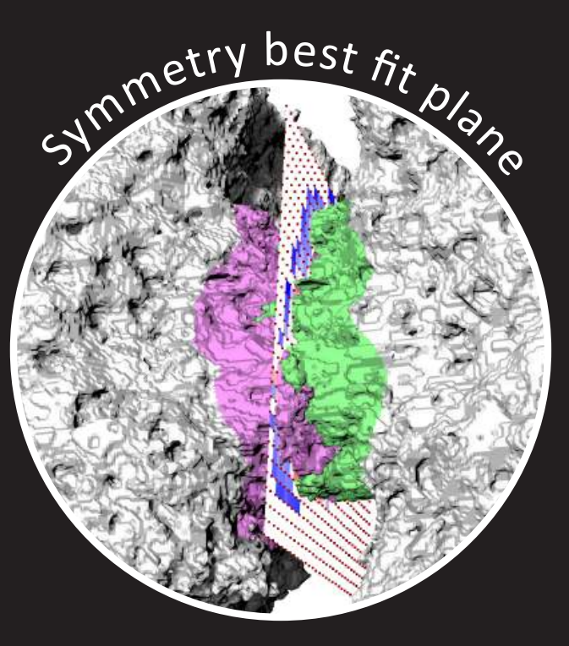

Red grid cells indicate intrusion (where the meshes breach the BFP), whereas blue grid cells indicate separation. The ratio of BFP and ITJ areas describes joint flatness, with values approaching 1.0 representing flatter surfaces)

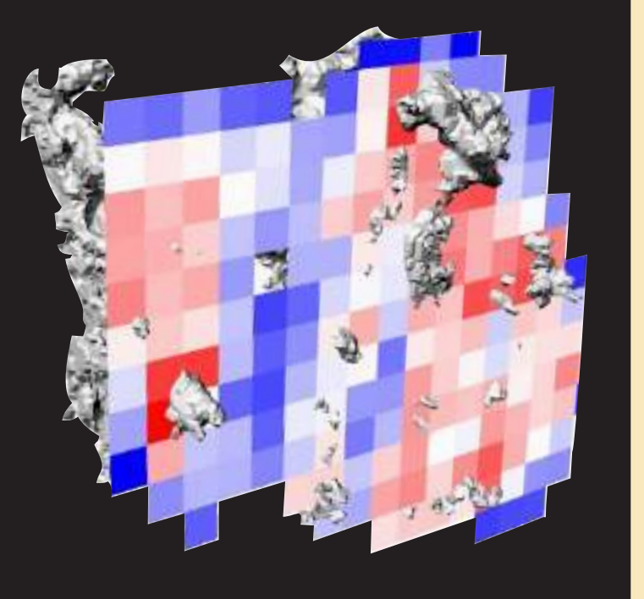

QUANTIFICATION OF TESSERAE INTERACTION

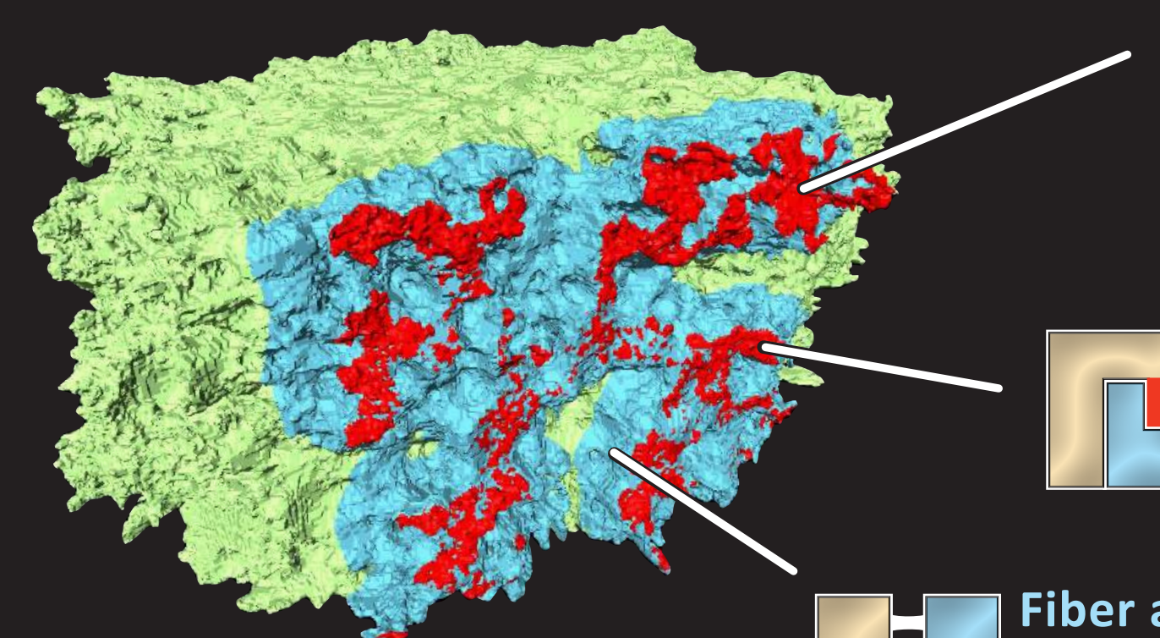

Intertesseral joint area
Area of T1: 140184 µm^2
Area of T2: 149346 µm^2
Ø: 144765 µm^2

Joint flatness
Flatness of T1: 0.6
Flatness of T2: 0.57
Ø: 0.59

Intrusion
Ø intrusion: 7.2 µm
Max. intrusion: 27 µm
= 41 % of BFP

Separation
Ø distance: 19.3 µm
Max. distance: 64,1 µm
= 23.3 % of BFP

Contact zone area
Area of T1: 19514 µm^2
Area of T2: 20789 µm^2
Ø: 20151 µm^2
= 13,92 % of ITJ

Interlocking area
835.7 µm^2
= 4,15 % of ICZ

Fiber attachment area
Area of T1: 120698 µm^2
Area of T2: 128586 µm^2
Ø: 124642 µm^2
= 86,1 % of ITJ

FINDINGS

Preliminary analyses of a tesseral neighbor-pair illustrate that, although the joint surfaces of tesserae have convoluted topographies (~0.6 flatness) with comparatively large intrusions into the joint space (up to 27µm), they are dominated by fibrous attachment areas (~86%), with only small regions (~14%) of neighbor contact including scant areas (~4%) of apparent interlocking. This suggests that in tessellated cartilage, unlike in other 'tiled' biological systems, interlocking plays little role in mechanics and the limited abutment of tesserae at contact zones may offer adequate skeletal stiffness in compression. These hypotheses will be tested via modeling work described in our 'Companion/Future Studies'.

Acknowledgements: We thank Aravind Jayasankar & Jacob Naumann for providing images and colleagues at the MPI for fruitful discussion on these topics. A Human Frontier Science Program Young Investigator's Grant (RGY0067) funded this work.